Accepted Manuscript

Title: Laser stabilization of GMAW additive manufacturing of Ti-6Al-4V components

Authors: Goncalo Pardal, Filomeno Martina, Stewart Williams

PII: S0924-0136(19)30165-7
DOI: https://doi.org/10.1016/j.jmatprotec.2019.04.036
Reference: PROTEC 16210

To appear in: *Journal of Materials Processing Technology*

Received date: 14 November 2017
Revised date: 23 April 2019
Accepted date: 26 April 2019

Please cite this article as: Pardal G, Martina F, Williams S, Laser stabilization of GMAW additive manufacturing of Ti-6Al-4V components, *Journal of Materials Processing Tech.* (2019), https://doi.org/10.1016/j.jmatprotec.2019.04.036

Laser stabilization of GMAW additive manufacturing of Ti-6Al-4V components

Goncalo Pardal[1], Filomeno Martina[1], Stewart Williams[1]

Welding Engineering and Laser Processing Centre - Cranfield University, Cranfield, Bedfordshire, MK43 0AL, United Kingdom

Corresponding author. Email: g.pardal@cranfield.ac.uk

Abstract:

GMAW (Gas Metal Arc Welding) of titanium is not currently used in industry due to the high levels of spatter generation, the wandering of the welding arc and the consequent waviness of the weld bead. This paper reports on the use of laser welding in conduction mode to stabilize the CMT (Cold Metal Transfer), a low heat input GMAW process. The stabilization and reshaping of Ti-6Al-4V weld beads was verified for laser hybrid GMAW bead on plate deposition. The laser beam was defocused, used in conduction mode, and was positioned concentric with the welding wire and the welding arc (CMT).

Finally, the results obtained for bead-on-plate welding were applied to an additively manufactured structure, in which a laser-hybrid stabilized sample was built and then evaluated against CMT-only sample. This work reveals that laser can be used to stabilize the welding process, improve the weld-bead shape of single and multiple layer depositions and increase the deposition rate of additive manufacture of Ti-6Al-4V from1.7 kg/h to 2.0 kg/h.

Keywords:

Laser welding, GMAW, stabilization, additive manufacturing, Ti-6Al-4V

Introduction:

Titanium is a metal highly used by the aerospace and aviation industries. These industries use very expensive subtractive techniques e.g. milling or turning to make final components, with loss of material of nearly 90% in swarf in some components (Allen, 2006).

A shift in this paradigm is being introduced by additive manufacturing techniques; these can increase the usage of titanium by adopting the layer-by-layer approach, thus eliminating or minimizing material waste. This paper is focused on trying to solve the issues with Gas Metal Arc Welding (GMAW) of titanium (Ti-6Al-4V), to introduce it as an alternative arc technology for the deposition of this material by Wire plus Arc Additive Manufacture (WAAM). This freeform metallic additive manufacturing process consists of using a welding process and a robotic manipulator to make near-net-shape components, layer by layer. WAAM can use several metallic alloys e.g. steel, aluminium, copper and Ti-6Al-4V to generate its final

components. As reported by (Williams et al., 2016) WAAM uses either Gas Tungsten Arc Welding (GTAW) (Bermingham et al., 2019) or Plasma Transferred Arc (PTA) (Mcandrew et al., 2018) for deposition of Ti-6Al-4V. The choice cannot fall on GMAW due to the instability, wandering and spatter generated by a GMAW arc when welding Ti-6Al-4V. TIG and PTA are effective techniques to deposit Ti-6Al-4V but they introduce extra considerations when compared with GMAW welding, the wire feeding is external, and so not coaxial, making it difficult to predict accurately the deposition path for complex parts. Moreover, these welding processes (PTA and GTAW) have a lower productivity (deposition rate) when compared with GMAW deposition. All of these disadvantages made the present investigation relevant to increase the productivity of WAAM, by combining GMAW with a laser in conduction mode to stabilize the arc.

Electric arc physics, in particular welding physics, have been studied for several years (Jüttner, 1997). The cathode spot is the main place where the current is transferred through an electric arc (Shinn et al., 2005). When GTAW is used for titanium, the cathode spot is located at the tungsten electrode. For this reason it is standard procedure to sharpen the electrode prior to welding to obtain a pointed tip to maintain the cathode spot restricted to this particular position (Guile, 1971). The fixed position of the cathode spot generates a stable weld without any arc wandering and spatter generation.

However, when GMAW is used, the polarity of the welding process is reversed and the cathode spot is now positioned on the titanium workpiece. Due to titanium's properties (boiling temperature, work function, thermal conductivity, and emissivity) being of intermediate magnitude, and the current density needed to transfer metal from the electrode to the baseplate, a thermionic welding arc with a cathode spot is generated at the workpiece (Shinn et al., 2005). Thermionic spots cover a broader area of the cathode, unlike non-thermionic cathodic spots like steel and aluminium, in which the arc is constricted to one or several highly-mobile spots, associated to enhanced evaporation. The welding arc has a single cathodic spot, with low period of oscillation, resulting in high level of instability and spatter generation to the deposited weld bead (Eagar, 1990).

To address the issue of cathode spot wandering and inconsistent metallic deposition in GMAW deposition of Ti, several approaches have been considered: changing the welding waveforms or using auxiliary processes to root the cathode spot, such as a laser.

(Li et al., 2001) used a modified active control to supress the spatter generated during pulsed GMAW of Ti. This control system consisted of a modified welding waveform, which uses a double-pulse of current that can detach the Ti droplet; this happens at lower levels of current when compared to traditional pulsed GMAW. Despite its success, this approach was only applicable to GMAW pulsed transfer, which generates higher heat-input than short-circuiting transfer. The higher heat-input can hinder the application of titanium welding to thin plates or some AM components. GMAW short-circuiting transfer was researched by (Sun et al., 2015) and was focused on droplet transfer in Cold Metal Transfer (CMT) on welding Ti-6Al-4V alloy. CMT is a low heat-input short-circuiting process that uses a reciprocating welding wire to control the droplet detachment into the weld pool. CMT has been successfully used as a deposition process to build WAAM components made of steel and aluminium (Kazanas et al., 2012) (Sun et al., 2015), showing that in principle CMT could be used to deposit Ti-6Al-4V too. However, the authors found the phenomenon of arc blow, i.e. when the cathode spot is relocated from the baseplate to the top of the deposited weld seam. Even though this issue

was overcome by increasing the travel speed of the deposition, such solution could not be applied to WAAM due to the geometrical constrains of the weld bead shape and process parameters to maintain a stable deposition (Martina et al., 2012).

(Li et al., 2009) studied high power hybrid laser-GMAW of commercially pure Ti and increased the productivity and mechanical properties of Ti welding, achieving a maximum welding speed of 9 m/min and a better combination of strength and ductility when compared to GMAW welding. Similar conclusions were found by (Murakami et al., 2012) with a maximum welding speed of 2 to 3 m/min when welding a single pass 6 mm thick commercially pure Ti; the authors also observed a strengthening effect in the joint. Hybrid laser-GMAW was not only investigated in terms of productivity increase and mechanical properties, but also to resolve the instability of GMAW welding (Denney et al., 2005). In the latter study, a Continuous Wave (CW) Nd:YAG laser was used at the leading edge of the weld pool to stabilize the GMAW cathodic spot. The laser power and beam diameter were varied, from 0.3 mm to close to 6 mm and from 200 W to 2000 W respectively to study the effect of each parameter on the stabilization of the cathode spot. The study showed that it was possible to use a CW laser to stabilize the weld bead deposition and to root the cathodic spot, preventing its lateral displacement and consequently prevent the waviness of the deposited weld bead. It was also shown that there is a minimum level of power density required to achieve the stabilization of the cathode spot and that this value is dependent on the laser beam diameter. This study was only for laser stabilization of Ti-6Al-4V welding, therefore no conclusions were drawn with regards to suitability for AM applications.

The present work explores the possibility of using a CW fibre laser to stabilize the CMT single and multiple-layer depositions of Ti-6Al-4V. CMT welding was chosen for the hybrid laser-arc welding process due to its current application in WAAM of steel and aluminium components. CMT is used in WAAM of steel and Al due to its low heat input and consequently distortions and relative high deposition rate when compared to PTA. In addition to the stabilization of the Ti deposition, the influence of the hybrid process (laser) on the geometrical aspects of the CMT weld beads and the possibility of application of this hybrid technique to manufacturing of WAAM components will be evaluated.

Experimental Procedure

The welding torch was perpendicular to the substrate and the contact tip to workpiece distance was maintained constant at 13.5 mm. The welding equipment used was a Fronius Trans pulse synergic 5000 power source with CMT mode selected. The welding arc parameters (voltage and current) and wire feed speed were monitored by a Triton Electronics AMV5000 real time weld analyser at a frequency of 5000 Hz. The collected data was post-processed to verify the stability of the welding process.

A Ti-6Al-4V welding wire of 1.2 mm diameter and matching 8 mm thick Ti substrate were used throughout the experimental work.

Table 1 - Wire and substrate chemical composition in weight percentage

	Ti	Al	V	Fe	O	C	N	H	Y
Wire	Bal	6.16	3.86	0.2	0.15	0.038	0.0079	0.0016	<0.0005
Substrate	Bal	6.28	4.13	0.13	0.13	<0.01	<0.01	0.006	<0.001

A CW IPG fibre laser with 8 kW of maximum power was used out of its focal position to achieve a 5 mm beam diameter.; The laser beam was concentric and aligned with the centre of welding arc (figure 1). The angle between the laser beam and the baseplate was set at 35°.

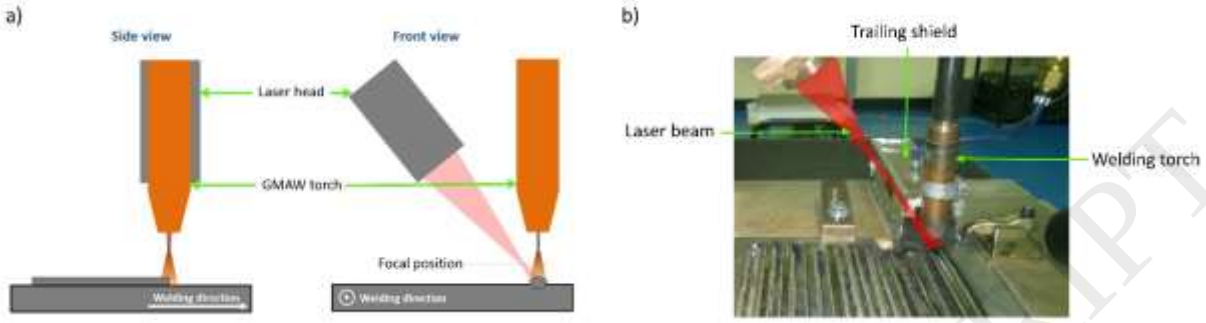

Figure 1 – Experimental setup of the hybrid laser-CMT welding process a) schematic representation, b) picture from the experimental setup.

A 200 mm long trailing shield, providing pure argon with a flow rate of 40 l/min, was attached to the CMT welding torch to prevent oxidation of the deposited metal.

Several hybrid laser-CMT bead on plate welds and multi-layer depositions were produced. The corresponding deposition parameters are shown in table 2.

Table 2 – Welding parameters for single layer and multilayer deposition.

Sample	Multilayer deposition	CMT welding		Laser welding		
		Travel speed (m/min)	Wire feed speed (m/min)	Beam diameter (mm)	Power (kW)	Power density (kW/cm^2)
1	No	0.5	9.0	5.0	0.0	-
2					1.0	5.1
3					1.5	7.6
4					2.0	10.2
5					2.5	12.7
6					3.0	15.3
7					3.5	17.8
8	Yes				0	-
9					2.5	12.7

The deposited samples (single and multiple layers) were sectioned and mounted in cold setting epoxy resin for metallographic analysis. These samples were then ground using an automatic grinding machine, using silicon carbide papers, and finally polished using a mixture of oxalic acid and a 0.04 µm suspension of colloidal silica. The samples were etched using hydrofluoric acid to enable observation of the microstructure and have better definition of the layering bands. The samples were observed under an optical microscope to evaluate their geometrical features.

Results:

Weld bead stability

The weld bead stability was determined by evaluating maximum and minimum deviations from the central line of each weld bead. The weld width changes with laser power therefore the relative waviness was calculated. The relative waviness was calculated by the difference between the maximum and the minimum point of waviness divided by the width of the weld bead.

Table 3 – Evaluation of the waviness of single layer deposition samples.

Sample	Weld width variation (mm)	Weld width (mm)	Relative waviness (%)
1	1.1	3.9	26.8
2	0.5	6.3	8.5
3	0.7	7.3	9.6
4	0.6	8.0	7.7
5	0.8	8.2	9.9
6	0.9	9.3	10.2
7	1.5	10.4	15.6

The waviness of the weld bead is a direct measurement of the wandering of the cathode spot and consequently of the instability of the welding process. Sample 1 (no laser) had the maximum relative waviness, whilst all of the hybrid samples had lower relative waviness. This demonstrates that the application of laser energy stabilizes the deposition, with a significant decrease in the relative waviness of the deposited metal.

The weld bead stability was also analysed based on the transient electrical waveforms obtained during deposition. Figure 2 shows the transient data from sample 1 for the interval of time between 5 and 5.5 seconds counting from the start of the deposition.

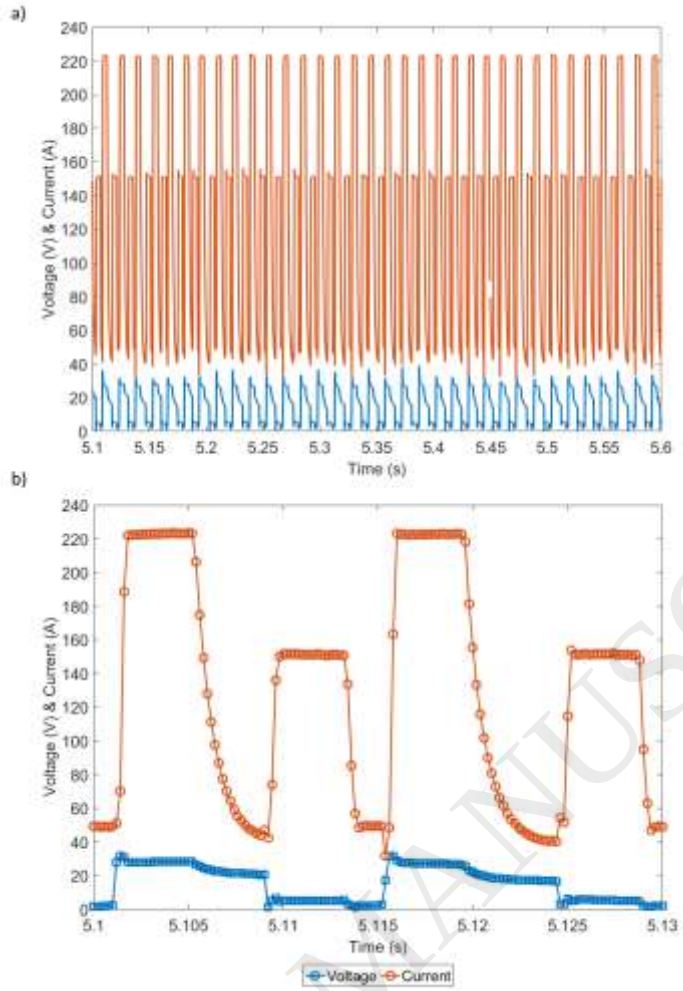

Figure 2 – Voltage and current transient waveform for sample 1 between 5 and 5.5 seconds a) and between 5.1 to 5.13 seconds b).

The CMT transient waveform is composed of two different pulses per cycle, one with lower current, corresponding to the short circuiting phase, and a second one where the current and voltage are higher during the arcing phase of the waveform. The same waveform pattern was also reported by (Sun et al., 2015) where the short circuiting increase in current was justified by the greater surface tension of Ti-6Al-4V when compared to steel. The stability of the CMT waveform was still acceptable without the use of any laser energy, however this was only true for a short section of the full transient data of the weld. To evaluate the stability of the full weld, scatter plots of the voltage and current were generated for all the transient points recorded for the entire weld bead.

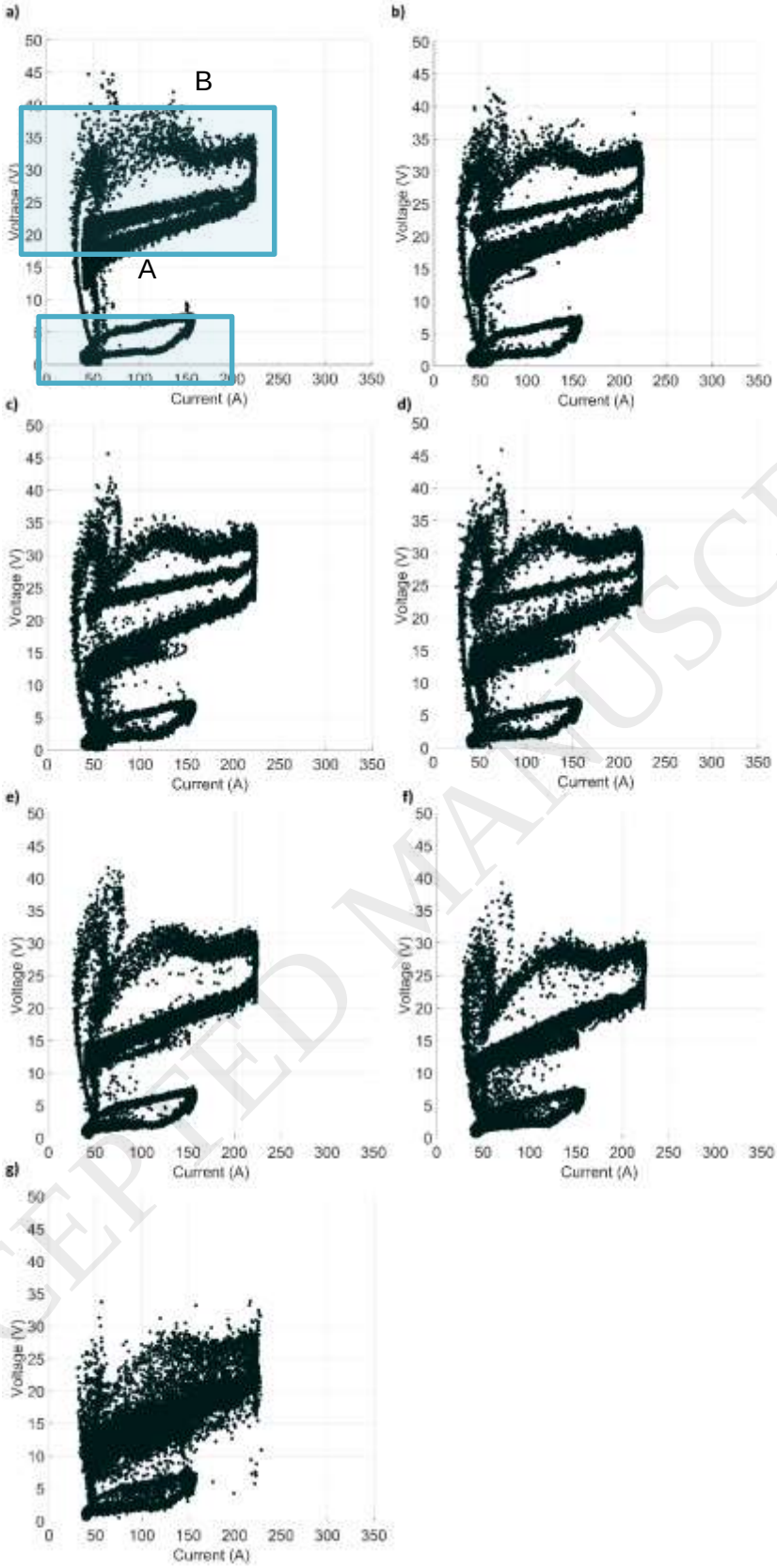

Figure 3 – Voltage and current scatter plots with the increase in laser power density a) 0 kW/cm^2, b) 5.1 kW/cm^2, c) 7.6 kW/cm^2, d) 10.2 kW/cm^2 e) 12.7 kW/cm^2, f) 15.3 kW/cm^{2}and g) 17.8 kW/cm^2.

These plots also show both phases of the waveform, short circuiting and arcing, depicted by the elliptical areas shown in the graph. The short circuiting phase has lower values of current and voltage and is depicted by the lower elliptical area of the plots (Figure 3 a – area A). The Arcing phase has higher values of current and voltage and so it is depicted in the voltage current plots by the elliptical area closer to the top of the graphs (Figure 3 a – area B). The plots reveal some instability in the two first welds due to the higher scatter in area B of (Figure 3 a) and b). This shows that either when the laser is not in use, or the laser energy is low, the welding process is not completely stabilized. With the increase of the laser power density, the instability disappears and the scatter in the plots is reduced, showing better stability of the arc parameters (Figure 3 c to f). The maximum voltage of the ellipse B decrease with the increase in laser power. When the power density increases to its maximum (Figure 3 g), the scatter plot loses the two elliptical shapes, showing the loss of stability of the process in the arcing phase of the waveform and an increase in spatter was also noticed in this particular sample. This could be due to the formation of a keyhole by the addition of the laser and arc energy.

The electrical instability match the wandering of the welding process in sample 1 and 7 (Figure 3 a) and g). However, sample 2 (Figure 3 b) shows some electrical instability that is not verified by the wandering of the weld bead. The same result was observed by (Shinn et al., 2005) who found the necessity of having a minimum of 7 kW/cm^2 of laser power density to stabilize the welded samples with a beam diameter between 3 and 5 mm.

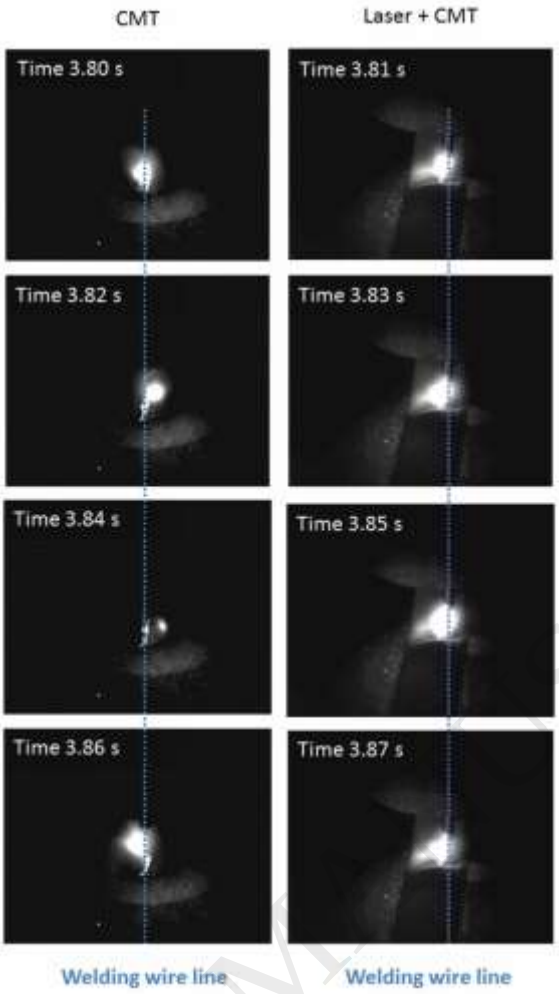

Figure 4 – Video frames from a non-stabilized CMT weld and a laser hybrid CMT weld.

Figure 4 shows images of samples from previous welds made as a preparation for this paper, they are not from the samples used in this paper. In these figures is possible to see the instability of the welding arc of a non-stabilized CMT welding arc, against a stabilized weld. The arc from the non-stabilized weld starts to the left of the welding wire line and finishes at 3.84s at the right of it, restarting again at its left. This captures the lateral displacement of the welding arc during the CMT process and the waviness present in the resulting welds. The laser hybrid weld shows a very stable welding arc and no lateral movement during the full weld bead, resulting into a stable weld with lower waviness. As the laser energy is added to the arc region an increase in the temperature field particularly at the centre of the weld pool generates a hot spot that roots the cathodic spot and consequently the welding arc stopping its lateral wandering

Weld bead geometry

The weld bead geometry of the welded samples was changed during the experimental trials, the minimum weld width was verified by sample 1 (CMT only sample) with 3.9 mm of width. Sample 7 (CMT + laser) was the wider sample with 10.4 mm of width (Table 3). There is an evolution of the sample width with the increase in laser power for all the samples while the beam diameter was kept constant as 5 mm. The evolution of the weld width with the increase of the power density shows that the laser beam diameter is not controlling the width of the

welded samples and it is power density or the total energy of the process that determines the weld width.

The energy values of the laser were calculated using the specific point energy:

$$E_{sp} = PD.t_i.Area_{beam} \quad (1)$$

Where E_{sp} is the specific point energy (J), PD is the laser power density (kW/cm^2), t_i the interaction time (s) and $Aarea_{beam}$ (mm^2) the area of the beam that irradiates the surface of the metal (Suder and Williams, 2011). The specific point energy is related to the full energy of the laser beam that is provided to the workpiece.

In order to give a comparison of both energies (laser and arc), for CMT the heat input was normalised using the same diameter as the laser beam, by multiplying the heat input by the laser beam diameter:

$$HI = \eta.\frac{60.VI}{1000v} * D_{beam} \quad (2)$$

Where HI is the heat input (J/mm), η is the efficiency of the welding process (for CMT the value is 0.85 used by (Pépe et al., 2011), V is voltage (V) and I is current (A), v is the travel speed (m/min) of the weld and the D_{beam} is the laser beam diameter.

Figure 5 shows how the energy within the laser spot area compares between the laser and the CMT processes, for different levels of laser power.

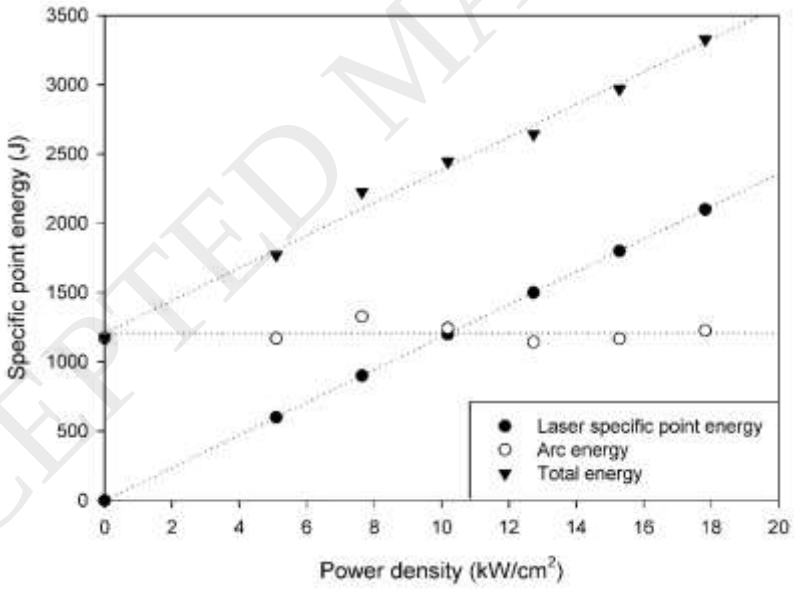

Figure 5 – Arc and laser energies used during the experimental trials.

The arc energy of the laser and CMT processes are similar when the laser power density is close to 10 kW/cm^2.

The weld bead shape is changed considerably since the first hybrid weld (5 kW/cm^2 of power density) showing that is possible to reshape the weld bead without any significant increase in the global energy values (Figure 6).

Besides affecting the weld width, the laser influenced also the weld bead shape; indeed there was a decrease in the weld bead's contact angle, revealing a better wetting of the substrate and, as shown before, also an increase in the width of the welded samples (figure 6).

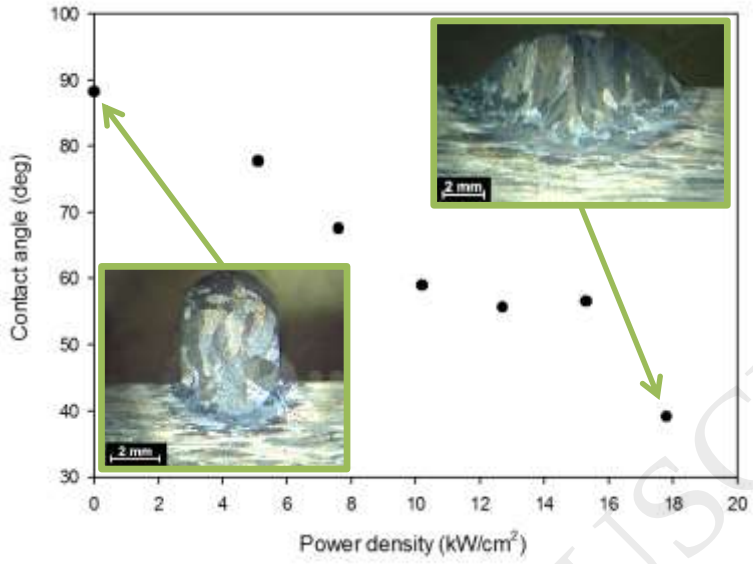

Figure 6 – Contact angle measured with the increase of laser power density, for single layer depositions.

As the laser power density increases, the heat affected zone also increases due to the higher energy added to the sample. This can be seen in the macros shown in figure 6.

Deposition rate

The cross-sectional area of the weld bead also increased with the increase of the laser energy. Due to the higher laser energy, there was an increase in the penetration area of the weld bead. However, a slight increase in the reinforcement area was also observed.

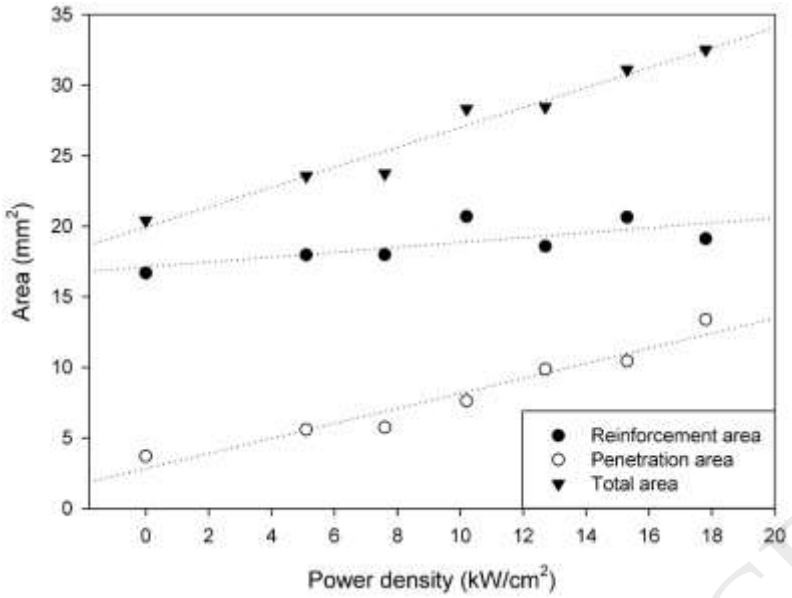

Figure 7 – Cross sectional areas (reinforcement, penetration and total) with the increase of laser power density.

This can only be explained by an increase in the wire feed speed automatically introduced by the welding power source, even though the wire feed speed was always set to the same value of 9 m/min. This automatic adjustment was caused by the increase in laser power density in the CMT + Laser hybrid process. The additional laser energy induced more melting of the Ti-6Al-4V welding wire and therefore, to obtain the short circuiting phase characteristic of the CMT welding process, the wire feed speed was automatically increased. This happens because the control of the CMT process is focused on the welding wire movement. This can be verified in Figure 8 where the measured wire feed speed and pulsing frequency are plotted against the laser power density used during the single layer deposition.

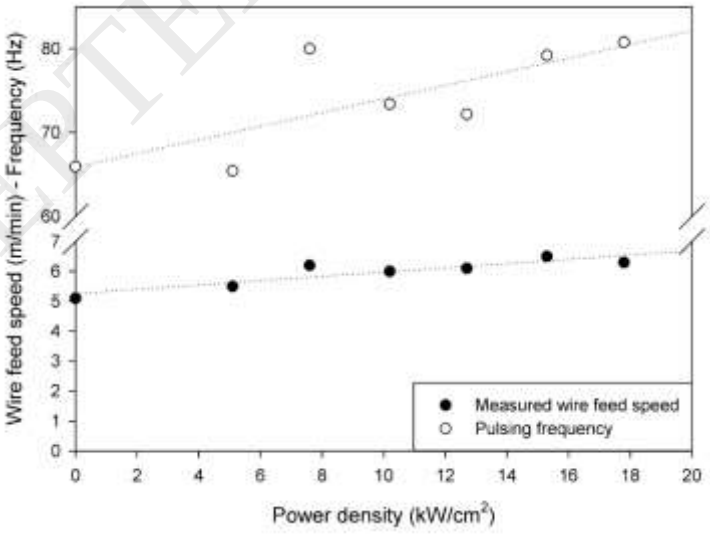

Figure 8 – Wire feed speed and frequency evolution vs laser power density.

Figure 8 reveals a good relationship between short circuiting frequency and measured wire feed speed.

As mentioned before, the introduction of the laser energy is reducing the voltage of the main arcing phase. As consequence, and to maintain good welding conditions, the power source is increasing the wire feed speed to cope with the changes in heat input transferred to the work piece, thus effectively increasing the deposition rate of the process. With the measured wire feed speed it is possible to calculate the deposition rate:

$$dep\ rate = 60.\rho.wfs.wwa$$

Where ρ is material density (kg/m^3), wfs is wire feed speed (m/min) and wwa is the welding wire cross sectional area (m^2). Using 4420 kg/m^3 as Ti-6Al-4V density the following plot can be generated.

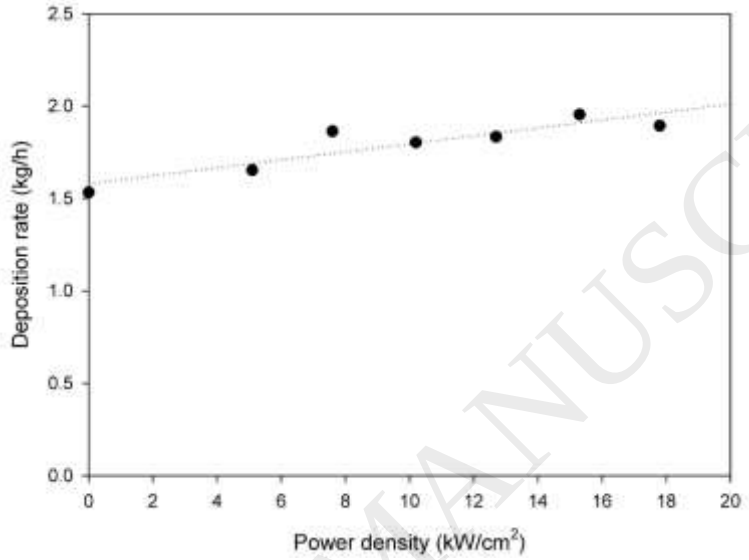

Figure 9 – Increase in deposition rate with the increase in laser power density.

As the deposition rate is calculated taking into account the measured wire feed speed, the graph shows the same trend observed in Figure 9. There was an increase in the deposition rate with the laser power density, in spite of identical set-values of the wire feed speed (9 m/min). The minimum deposition rate of 1.53 kg/h was obtained for simple CMT welding process; the maximum deposition rate of 1.95 kg/h was obtained for the hybrid process using a power density of 15.3 kW/cm^2 (+27%). This is result can be compared with the results obtained by (Martina et al., 2012) who used PTA to obtain a maximum deposition rate of 1.8 kg/h.

Multiple layer deposition

The same approach was applied for multiple layer deposition to understand if the same results were obtainable for the additive manufacturing of Ti-6Al-4V. Two walls were built with the parameters shown in table 2 (samples 8 and 9). Figure 10 shows that the deposition and heat input parameters were very consistent during multiple layer deposition.

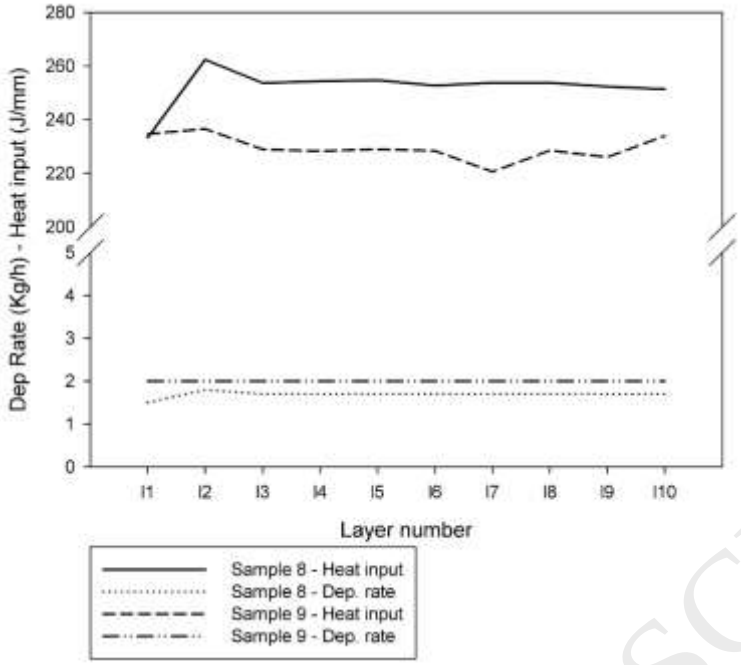

Figure 10 – Deposition rate and CMT heat input for each layer of the multiple layer deposited samples (Sample 8 and 9).

The multilayer depositions demonstrate once again that the variation in deposition rate by the hybrid laser-CMT welding is not due to changes in the arc heat input. Sample 9 (hybrid process) had an average of 10% lower arc heat input, however its deposition rate is 18% higher than sample 9.

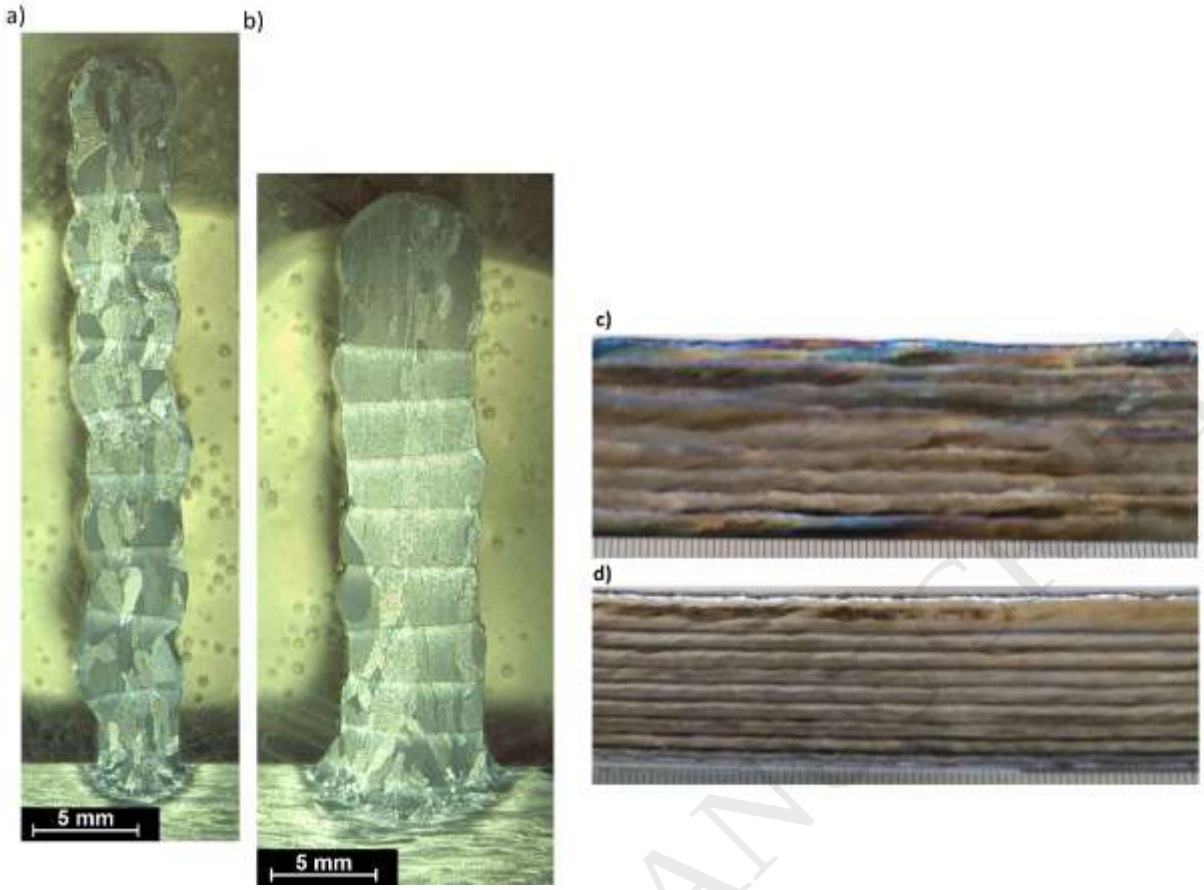

Figure 11 – Cross sectional metallographic samples and side views for a) and c) multilayer CMT deposition and b) and d) multilayer CMT laser hybrid deposition.

Figure 11 a) shows the typical waviness due to arc wandering in CMT welds in all of the deposited layers. On the other hand figure 9 b) shows a stable deposition in all of the deposited layers. The waviness present at the side of the wall in figure 9 a) is the main reason why CMT welding is not used in WAAM, as it decreases the effective wall width (Kazanas et al., 2012). After machining, the maximum width of the wall that could be produced by CMT process would be considerably less than that of the wall produced by hybrid laser-CMT (figure 9b). It would only be possible to obtain an effective wall width of 2.9 mm from a maximum wall width of 6.1 mm for the CMT wall Figure 10 a), while it would be possible to extract an effective wall of 5.9 mm from a 7.2 wall width for the hybrid wall. This shows an efficiency of 48% for the CMT deposition against an 82% efficiency for the hybrid wall. The dimensions of both walls are different even though the CMT parameters used were similar. The wall that was stabilized by the laser has lower height and is wider than the non-stabilized wall. This can be explained once again by the higher combined heat input of the hybrid laser-CMT building process compared to that of the single CMT process. The presence of columnar grains at the cross-section of the wall produced by hybrid laser-CMT process reflects the higher heat input present during this build. (Donoghue et al., 2016) observed a correlation between the columnar grains and the heat flow for WAAM process of Ti-6Al-4Al.

Conclusions:

This work shows that not only it is possible to stabilize a CMT weld of titanium using a fibre laser in conduction mode, but it is also possible to change the geometry and increase the deposition rate of the CMT process. This work also shows that all the above characteristics found for single layer process are also transferable to multiple layer deposition.

In summary the main findings of this work are:

- The stabilization of CMT welding of Ti-6Al-4V can be achieved by using a laser concentric with the arc and defocused on the substrate;
- The concentricity of the laser beam and the welding wire can simplify the tool path creation for AM manufacturing when compared with off-axis deposition methods as PTA.
- The hybrid laser-CMT process can be used to modify the weld bead shape or geometry of the deposited metal for single and multiple layer deposition;
- The deposition rate of the CMT increased by 27% when the laser is added into the process.
- WAAM of hybrid CMT has an increase in efficiency from 48% to 82% when compared with CMT WAAM of Ti-6Al-4V.

Acknowledgments:

The research covered in this paper was funded by the Engineering and Physical Sciences Research Council (EPSRC), in the HiDepAM project Grant n. EP/K029010/1 and also by the EPSRC Centre for Innovative Manufacturing in Laser-Based Production Processes Grant n. EP/K030884/1

References

Allen, J., 2006. An Investigation into the Comparative Costs of Additive Manufacture vs . Machine from Solid for Aero Engine Parts.

Bermingham, M.J., Stjohn, D.H., Krynen, J., Tedman-jones, S., Dargusch, M.S., 2019. Acta Materialia Promoting the columnar to equiaxed transition and grain re fi nement of titanium alloys during additive manufacturing. Acta Mater. 168, 261–274. doi:10.1016/j.actamat.2019.02.020

Denney, P.E., Shinn, B.W., Fallara, P.M., 2005. Laser Plus GMAW Hybrid Welding of Titanium, in: Proceedings of The Fifteenth (2005) International Offshore Ans Polar Engineering Conference. pp. 106–111.

Donoghue, J., Antonysamy, A.A., Martina, F., Colegrove, P.A., Williams, S.W., Prangnell, P.B., 2016. The effectiveness of combining rolling deformation with Wire-Arc Additive Manufacture on ??-grain refinement and texture modification in Ti-6Al-4V. Mater. Charact. 114, 103–114. doi:10.1016/j.matchar.2016.02.001

Eagar, S.T.E. and T.W., 1990. Characterization of Spatter in Low-Current GMAW of Titanium Alloy Plate. Weld. J. 382s–388s.

Guile, A.E., 1971. Arc-Electrode Phenomena. Proc. Inst. Electr. Eng. 118, 1131. doi:10.1049/piee.1971.0246

Jüttner, B., 1997. Properties of Arc Cathode Spots. Le J. Phys. IV 07, C4-31-C4-45. doi:10.1051/jp4:1997404

Kazanas, P., Deherkar, P., Almeida, P., Lockett, H., Williams, S., 2012. Fabrication of geometrical features using wire and arc additive manufacture. Proc. Inst. Mech. Eng. Part B J. Eng. Manuf. 226, 1042–1051. doi:10.1177/0954405412437126

Li, C., Muneharua, K., Takao, S., Kouji, H., 2009. Fiber laser-GMA hybrid welding of commercially pure titanium. Mater. Des. 30, 109–114. doi:10.1016/j.matdes.2008.04.043

Li, P.J., Li, P.J., Shang, Y.M., Shang, Y.M., 2001. Modified Active Control of Metal Transfer and Pulsed GMAW of Titanium. Weld. J. 80, 54–61.

Martina, F., Mehnen, J., Williams, S.W., Colegrove, P., Wang, F., 2012. Investigation of the benefits of plasma deposition for the additive layer manufacture of Ti-6Al-4V. J. Mater. Process. Technol. 212, 1377–1386. doi:10.1016/j.jmatprotec.2012.02.002

Mcandrew, A.R., Alvarez, M., Colegrove, P.A., Hönnige, J.R., Ho, A., Fayolle, R., Eyitayo, K., Stan, I., Sukrongpang, P., Crochemore, A., Pinter, Z., 2018. Interpass rolling of Ti-6Al-4V wire + arc additively manufactured features for microstructural re fi nement. Addit. Manuf. 21, 340–349. doi:10.1016/j.addma.2018.03.006

Murakami, T., Nakata, K., Yamamoto, N., Liao, J., 2012. Formation of One Pass Fully-Penetrated Weld Bead of Titanium Plate by Fiber Laser and MIG Arc Hybrid Welding. Mater. Trans. 53, 1017–1021. doi:10.2320/matertrans.M2012044

Pépe, N., Egerland, S., Colegrove, P.A., Yapp, D., Leonhartsberger, A., Scotti, A., 2011. Measuring the process efficiency of controlled gas metal arc welding processes. Sci. Technol. Weld. Join. 16, 412–417. doi:10.1179/1362171810Y.0000000029

Shinn, B.W., Farson, D.F., Denney, P.E., 2005. Laser stabilisation of arc cathode spots in

titanium welding. Sci. Technol. Weld. Join. 10, 475–481. doi:10.1179/174329305X46673

Suder, W., Williams, S., 2011. Use of fundamental laser material interaction parameters in laser welding. CLEO 2011 - Laser Sci. to Photonic Appl. 24, 1–2. doi:10.2351/1.4728136

Sun, Z., Lv, Y., Xu, B., Liu, Y., Lin, J., Wang, K., 2015. Investigation of droplet transfer behaviours in cold metal transfer (CMT) process on welding Ti-6Al-4V alloy. Int. J. Adv. Manuf. Technol. 80, 2007–2014. doi:10.1007/s00170-015-7197-9

Williams, S.W., Martina, F., Addison, A.C., Ding, J., Pardal, G., Colegrove, P., 2016. Wire + arc additive manufacturing. Mater. Sci. Technol. 32, 641–647. doi:10.1179/1743284715Y.0000000073

2019-04-26

Laser stabilization of GMAW additive manufacturing of Ti-6Al-4V components

Pardal, Goncalo

Elsevier

Goncalo Pardal, Filomeno Martina and Stewart Williams. Laser stabilization of GMAW additive manufacturing of Ti-6Al-4V components. Journal of Materials Processing Technology, Volume 272, October 2019, Pages 1-8

https://doi.org/10.1016/j.jmatprotec.2019.04.036